Applied Catalysis A, General 648 (2022) 118920

Contents lists available at ScienceDirect

Applied Catalysis A, General

journal homepage: www.elsevier.com/locate/apcata

Oxidation of glucose to glycolic acid using oxygen and pyrolyzed spent Li-ion battery electrode material as catalyst

Ananda S. Amarasekara [a,b,*], Hashini N.K. Herath [a], Tony L. Grady [a], Cristian D. Gutierrez Reyes [c]

[a] Department of Chemistry, Center for Energy and Environmental Sustainability Prairie View A&M University, 700 University Drive, Prairie View, TX 77446, USA
[b] Center for Energy and Environmental Sustainability Prairie View A&M University, 700 University Drive, Prairie View, TX 77446, USA
[c] Department of Chemistry and Biochemistry, Texas Tech University, 3122 Main Street, Lubbock, TX 7940, USA

ARTICLE INFO

Keywords:
Glucose
Glycolic acid, Li-ion batteries
Lithium nickel manganese cobalt oxide
Oxidation catalyst

ABSTRACT

A search for non-noble catalysts for biomass processing led to the discovery that pyrolyzed electrode coating of spent Li-ion batteries can be used as an excellent catalyst for oxidation of D-glucose to glycolic acid. New no/low-cost catalyst was prepared by pyrolyzing black electrode coatings of 18,650 Li-ion cells from a spent DELL 1525 laptop battery at 600 °C. Catalyst was characterized using SEM, EDX and X-ray and was shown to contain lithium nickel manganese cobalt oxide ($Li_aNi_bMn_cCo_dO_e$) on carbon with Ni: Mn: Co 4.12: 2.10: 1.50. The catalytic activity of this material was evaluated for oxidation of D-glucose in aq. NaOH and water; glycolic, tartaric, malic, succinic and 2-hydroxybutaric acid were identified as key degradation products. The highest glycolic acid yield of 94% was obtained for oxidation of D-glucose under 3.4 Atm. oxygen, 120 °C, 2.0 h in 0.5 M aq. NaOH using 10 g catalyst/mol glucose.

1. Introduction

Chemical and biochemical transformations of D-glucose is a rational approach to produce value added renewable carbon based chemical feed stocks and fuels, given that D-glucose is the most abundant monosaccharide, which occurs as its linear polymeric form cellulose [1], [2], [3]. Oxidation of D-glucose with or without fragmentation is one of the most widely studied reactions for processing this C-6 building block [4], [5]. Controlled D-glucose oxidation can be achieved by using strong oxidants like nitric acid, oxygen or air in the presence of catalysts and electrochemical as well as enzymatic methods. These oxidation processes are known to give a broad range of C1 to C6 value added oxidation products and some of the common oxidation products include: formic, lactic, glycolic, succinic, tartaric, gluconic, glucaric and glucuronic acids [6], [7].

Classical chemical glucose oxidation reactions commonly use stoichiometric strong oxidants such as sodium hypochlorite, sodium periodate, hydrogen peroxide or nitric acid; these oxidants are expensive, polluting and often accompanied by large amounts of side products [8], [9], [5]. On the other hand enzymatic and catalytic oxidations are more selective and efficient, in particularly, heterogeneous catalysts are generally recyclable and environmentally benign in achieving sustainable carbohydrate biorefineries. However, conventional heterogeneous catalysts used in D-glucose oxidation reactions are expensive noble metals such as, Au [10], [11], Pt [7], [12], Pd [13] or Au, Pt, Pd nanoparticles [14], [15], [16], [17] as well as bimetallic systems; Au-Pd [18], Au-Pt [19], [18], Pt-Cu [6], Pd-Rh [20], Au-Pt, Au-Rh nano particles [21], [22]. Therefore, the catalyst cost is a major disadvantage in currently available D-glucose oxidation technologies. Although, in recent years a few researchers have achieved a limited success in using non-noble metal catalysts for oxidation of D-glucose, these reactions are invariably photo-oxidations or electrochemical methods with numerous challenges in scaling up to industrial processes [23], [24]. For example, Cao et al. recently reported the preparation of a new non-noble metal, NiCuO electro-catalyst with flower-like nanostructure for efficient oxidation of glucose under mild conditions [25]. In another example, Lopez-Sanchez and co-workers have shown that Ag nanoparticles supported on TiO_2 can be used as a photo catalyst for the visible-light mediated oxidation of D-glucose to gluconic acid, arabinose, erythrose, glyceraldehyde and formic acid [26]. Furthermore, transition metal catalyzed oxidation of polyols is a widely studied reaction; for instance, Yan et al. have reported a microcrystalline α-Mn_2O_3 catalyzed

---

* Corresponding author.
E-mail address: asamarasekara@pvamu.edu (A.S. Amarasekara).

https://doi.org/10.1016/j.apcata.2022.118920
Received 27 June 2022; Received in revised form 4 October 2022; Accepted 18 October 2022

oxidation of glycerol to glycolic acid [27]. In another example, same research group reported the selective oxidation of C_2–C_4 polyols to corresponding primary hydroxy acids using PO_4^{3-} co-ordinated Pt as the catalyst [28]. Consequently, there is a clear potential for non-noble metal catalyzed oxidation of D-glucose to value added products. Therefore, as a part of our research efforts on development of industrially feasible catalytic methods for processing renewable feedstocks we have instigate a search for inexpensive non-noble metal catalysts for carbohydrate oxidation reactions [29], [30], [31], [32]. Under this project we have developed a new catalyst system from a waste product: spent Li-ion battery black electrode material as a minimal or no cost catalyst for oxidation of D-glucose to a valuable hydroxy acid, glycolic acid used in skin-care formulations, cosmetic, textile, polymer, food and in many other industries [33], [34], [35].

The rapid expansion in the use of Li-ion batteries (LiBs) for electrical energy storage has resulted an accumulation of spent LiBs as a waste product. The assessment of global stockpile of discarded LiBs is a challenging task, but a 2017 estimate by Guo et al. predicted that about 400 million tons of LiBs are expected to reach end of life by 2020 [36]. These statistics signify that used LiBs are among the fastest growing waste streams that contain high levels of critical metals Li, Ni, Mn and Co [37]. These metals, due to their high concentrations in batteries that exceeded the limits set by environmental protection agencies are toxic and pose considerable threats to the environments if untreated [38]. To minimize the undesirable environmental impacts as well as to recover valuable critical materials from them, a number of end-of-life management approaches have been developed. These technologies are based on pyrolysis, biochemical or enzymatic methods as well as hydro-metallurgical process [37], [38], [39], [40], [41]. Recycling graphite carbon and expensive metals: Li, Ni, Mn and Co as well as Cu and Al from electrodes of spent batteries is an essential step in wider use of LiBs. Nevertheless, the recycling of these elements for manufacturing of new batteries requires separation of metals from carbon and binders as well as difficult isolation of each element in the form of pure compounds. Therefore, re-purposing Li, Ni, Mn and Co in spent LiBs as a pre-fabricated catalyst is an attractive suggestion since Co, Mn, Ni oxides are renowned for their catalytic properties, especially for oxidation reactions [42], [43]. As far as we are aware, there is only a handful of reports on the use this precious waste material as a catalyst; where it was used only as a reduction catalyst for electrochemical oxygen reduction and carbonyl group reduction [44], [45], [46]. Interestingly, it is not necessary to immobilize the active centers on a solid support, as Ni, Mn and Co oxides are already impregnated on graphite carbon in this low or no-cost heterogeneous catalyst. In this communication we present the preparation of a novel carbohydrate oxidation catalyst by pyrolysis of electrode coating material collected from a used laptop battery and application of this catalyst for the oxidation of D-glucose under oxygen atmosphere to produce value added glycolic acid in excellent yield.

2. Experimental

2.1. Materials and instrumentation

ACS grade tartaric, malic, glycolic, succinic, oxalic and 2-hydroxy butyric acids, D-glucose (>99%), sodium hydroxide, sulfuric acid (98%) were purchased from Aldrich Chemical Co. Compressed oxygen (99.9%) was from Airgas. A spent DELL 1525 laptop battery (87 Wh, 11.1 V) was used in collecting Li-ion battery black material (LiBBM). Attenuated total reflection infrared (ATR-IR) spectra were recorded in the 500–4000 cm^{-1} range on a Smiths IdentifyIR spectrometer with a diamond ATR (Danbury, CT, USA). Thermogravimetric analysis (TGA) were carried out using a Perkin Elmer - Diamond High Temp 115 instrument; Pt crucibles, 25–800 °C in air, scanning rate: 10 °C/min. LiBBM samples were pyrolyzed in air by placing inside a 12 mm × 200 mm quartz tube horizontally placed in a Lindberg Blue M Mini-Mite tube furnace (Thermo Scientific). Catalyst was powdered using Bel-Art SP Science ware Micro-Mill™ II Grinder. FEI Quanta 400 ESEM instrument was used for Scanning Electron Microscopy (SEM) and imaging was performed with a secondary electron detector at an accelerating voltage of 20 kV. Powder X-ray spectrograph was collected on a Shimadzu, XRD-7000 Maxima instrument. All high pressure reactions under oxygen atmospheres were carried out using a Parr Instrument Co. reactor with a 50 mL 4720 stainless-steel pressure vessel, 4838 reactor temperature controller, pressure gauge and without stirring.

2.2. LC-MS analysis

The samples were separated on a C18 column (Thermo Sci; Accucore Vanquish C18 150 mm × 2.1 mm, 100 Å, 1.5 μm) using an UltiMate 3000 Nano UHPLC system (Thermo Sc., San Jose, CA). The output was analyzed on a TSQ Vantage (Thermo Sc., San Jose, CA) triple quadrupole mass spectrometer. Data-dependent acquisition mode (DDA) with a full scan event at a range of 40 – 300 m/z in Q3 with a scan time of 0.7 s and peak width of 0.7 FWHM was performed in negative ion mode. The chromatographic conditions of mobile phase A (MPA) was 98% HPLC water, 2% methanol with 0.1% of formic acid and 2 mM ammonium formate; mobile phase B (MPB) was 99% methanol, and 1% water with 0.1% of formic acid and 2 mM ammonium formate. A multistep gradient with a flow rate of 0.15 mL/min and a temperature of 40 °C was used for the separation, where MPB was 5% for 8 min. It was increased to 60% after 10 min and kept constant until 10 min. Later, it was decreased to 5% in 2 min and maintained in the same condition until 16 min to equilibrate the column. Before analysis the signal of the standards were identified according to their precursor charge state $[M-H]^{-1}$: 148.9, 89.0, 132.9, 74.9, 116.9, and 103.1 for tartaric, oxalic, malic, glycolic, succinic and 2-hydroxy butyric acid respectively. The precursor signals for the investigated standards were confirmed with PubChem® database in LC-ESI-QQ mode. Three micro liters of the standard and sample solutions were injected in triplicate, the precursor signals were extracted and the peak area of the signals calculated using Xcalibur Qual Browser software.

2.3. Preparation of LiBBM-600 catalyst

A spent DELL 1525 laptop battery (87 Wh, 11.1 V) was discharged by complete immersing in a 10% aqueous sodium chloride solution at room temperature for 5 days. Then repeatedly washed with deionized water, dried with paper towels and the casing was opened to collect nine 18650 cells, which were dismantled to collect black coatings on Cu anode and Al cathode foils. The combined black powder was air dried at room temperature for 3 days to give 43.45 g of Li-ion battery black electrode coating material (LiBBM) (Fig. 1). A 10 mg sample of LiBBM was analyzed using thermogravimetric analysis (TGA) and the thermogravimetry curve is shown in Fig. 2. As volatile binders and residual electrolytes are evaporated by heating above 600 °C in air a 20.0 g of LiBBM was subjected to a preparatory scale pyrolysis using Lindberg Mini-Mite tube furnace for 30 min in air. The pyrolyzed product was cooled to room temperature, grounded in a Bel-Art SP Science ware Micro-Mill™ II Grinder, sieved through mesh size 25 (710 μm) to give 15.12 g fine black powder, stored in an air-tight bottle till use, named as LiBBM-600 and characterized using ATR-IR, SEM, EDX and powder X-ray and these spectrographs are shown in Figs. 3, 4 and 5.

2.4. General procedure for oxidation of D-glucose using LiBBM-600 catalyst under oxygen atmosphere

A mixture of D-glucose (396 mg, 2.00 mmol), LiBBM-600 catalyst (20 mg), 2.00 mL of 1.0 M aqueous sodium hydroxide and 2.00 mL of deionized water was prepared in a 50 mL Parr reactor. The reactor was closed and flushed with oxygen three times to remove air and pressurized to 1.00 – 3.40 Atm. with oxygen, heated to the desired temperature and maintained at this temperature using 4838 reactor temperature

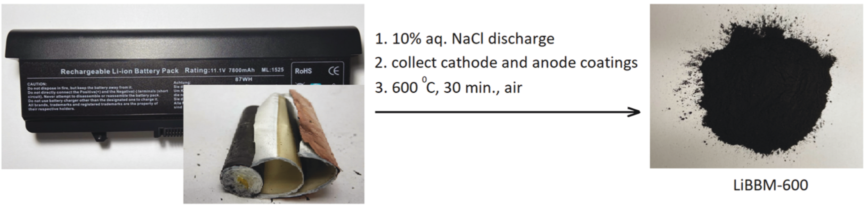

Fig. 1. Preparation of LiBBM-600 catalyst from spent DELL 1525 laptop battery.

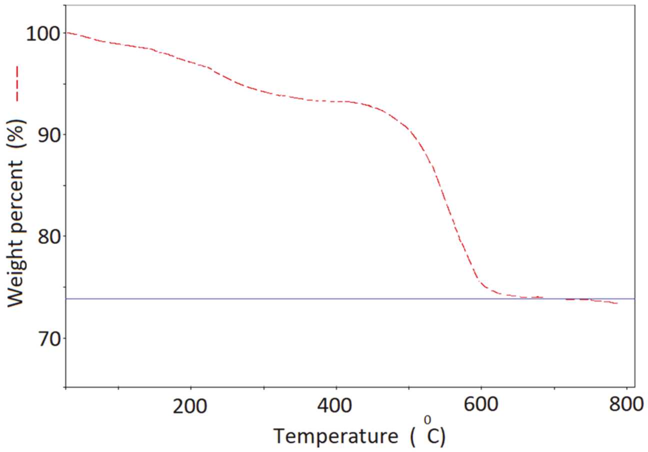

Fig. 2. Thermogravimetric analysis of LiBBM.

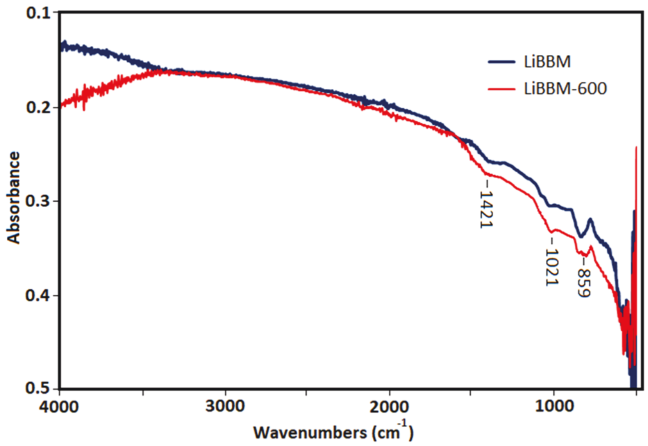

Fig. 3. Attenuated total reflection infrared (ATR-IR) spectra of LiBBM and LiBBM-600.

controller with ± 1 °C accuracy. Then reactor was cooled to room temperature, acidified to pH = 2 with 1 M H_2SO_4 and diluted to 10.00 mL with deionized water. The contents were transferred into a centrifuge tube and centrifuged at 1700 g for 15 min to remove the catalyst. The clear supernatants were analyzed using LC-MS after filtering through a 0.22 μm hydrophobic micro filter and products were identified by comparison of retention times, confirmed with mass spectra and quantified using peak areas of authentic samples as described in Section 2.2. The reaction conditions, conversion (%) and product yield (%) in LiBBM-600 catalyzed oxidation of D-glucose are shown in Table 1.

Conversion (%) and product yield (%) were calculated using equations:

$$\text{Conversion}(\%) = \frac{\text{mol of glucose used} - \text{mol of glucose unreacted}}{\text{mol of glucose used}} \text{x}100\%$$

$$\text{Product yield}(\%) = \frac{\text{mol of product detected}}{\text{mol of glucose used}} \text{x}100\%$$

3. Results and discussion

3.1. Preparation of LiBBM-600 catalyst and characterization

Black electrode coatings on copper anode and aluminum cathode foils of 18650 cells from a spent DELL 1525 laptop battery was pyrolyzed at 600 °C to prepare the LiBBM-600 catalyst. A sample of combined cathode and material, LiBBM was first subjected to thermogravimetric analysis to determine the pyrolysis temperature and this TGA profile is shown in Fig. 2. TGA of LiBBM shows two major weight loss steps, the first around 260 °C and the second larger loss around 550 °C; the weight is relatively stable after 600 °C, most likely indicating the loss or evaporation of binders such as carboxymethyl cellulose and styrene butadiene copolymer as well as residual liquid electrolytes, after reaching approximately 600 °C; leaving a 74% residual weight corresponds to LiBBM-600. Therefore, the preparatory scale product of 15.12 g of LiBBM-600 from 20.00 g of LiBBM at 75.6% yield is reasonable.

In an attempt to study the effect of pyrolysis of LiBBM at 600 °C for 30 min in air, we have compared the attenuated total reflection infrared (ATR-IR) spectra of LiBBM and LiBBM-600, and these spectra are in Fig. 3. The IR spectra is comparable to typical graphite spectrum and the broad peak at 1421 cm^{-1} may be due to the C-O absorption of a very small fraction of oxidized carbons in graphite [47]. The intensity of this broad peak as well as the other smaller peaks at 1021 and 859 cm^{-1} does not show significant changes due to pyrolysis indicating that graphite in LiBBM is not oxidized further due to pyrolysis.

Scanning electron microscopy (SEM) and Energy Dispersive X-ray Spectroscopy (EDX) analyses of LiBBM-600 are shown in Fig. 4a and b respectively. The SEM image shows irregular metallic and or metal oxide particles with clusters of about 5 μm in diameter and smaller particles less than 1 μm in size. The Energy Dispersive X-ray Spectroscopy (EDX) analyses show peaks for elements: C, O, Ni, Mn, Co, Al and P in the plot in Fig. 4b and the table below. However, Li expected is not observed, as EDX is not sensitive to Li. The Al in the LiBBM-600 sample may be due to a contamination from aluminum foil used in cathode and P is probably from residual electrolyte. The presence of elements: Ni, Mn and Co in LiBBM-600 is most likely due to the use of lithium nickel manganese cobalt oxide ($Li_aNi_bMn_cCo_dO_e$), the active material employed in the DELL 1525 laptop battery used in this study. Furthermore, the empirical composition of these elements is in the ratio: Ni: Mn: Co 4.12: 2.10: 1.50 as indicated in the EDS data shown in Table in Fig. 4b.

The X-ray diffraction pattern of LiBBM-600 is shown in Fig. 5, and this diffractogram is comparable to other typical LiB cathode material X-ray data reported in the literature [48]. The strong peaks at 2θ= 26.47° and 44.49° can be assigned to graphite carbon, which is the major component in the heterogeneous sample [46]. The smaller peaks at 2θ= 18.59°, 31.82°, 36.40° and 38.53° can be assigned to $LiMO_2$ type

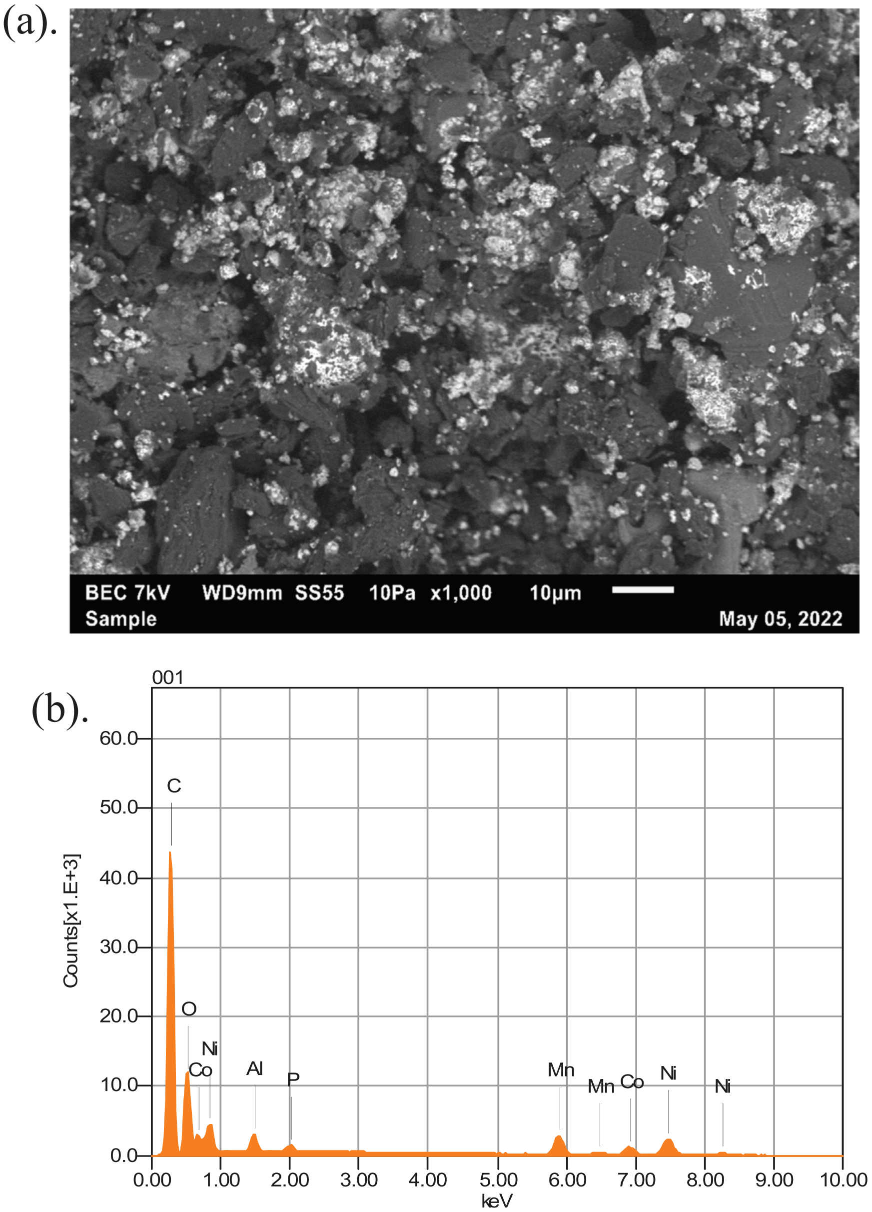

Element	Mass %	Atom %
C	57.24	77.31
O	14.07	14.26
Al	0.80	0.48
P	0.43	0.23
Mn	7.12	2.10
Co	5.43	1.50
Ni	14.90	4.12
Total	100.00	100.00

Fig. 4. (a) Scanning electron microscopy (SEM) and (b) Energy Dispersive X-ray Spectroscopy (EDX) analyses of LiBBM-600.

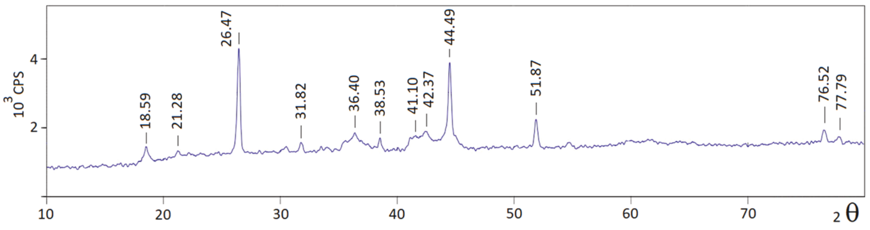

Fig. 5. Powder X-ray diffractogram of LiBBM-600.

Table 1
Reaction conditions, conversion (%) and product yields (%) in LiBBM-600 catalyzed oxidation of D-glucose under oxygen atmosphere. All reactions were carried out with 2.00 mmol of D-glucose, 20 mg of LiBBM-600 catalyst.

Entry	Reaction conditions	Conversion (%)	Yield (%)				
			GA	TA	MA	SA	HBA
1	150 °C, 2 h, 3.4 Atm. O_2; 0.50 M NaOH	100	78	2	–	2	–
2	150 °C, 6 h, 3.4 Atm. O_2; 0.50 M NaOH	100	42	2	–	10	–
3	140 °C, 4 h, 3.4 Atm. O_2; 0.50 M NaOH	100	52	3	–	9	
4	130 °C, 4 h, 3.4 Atm. O_2; 0.50 M NaOH	100	66	3	–	5	
5	120 °C, 2 h, 3.4 Atm. O_2; 0.50 M NaOH	100	94	1	–	2	–
6	100 °C, 2 h, 1.0 Atm. O_2; 0.50 M NaOH	100	85	3	1	–	2
7	100 °C, 2 h, 1.0 Atm. O_2; water	12	5	2	–	–	–

oxides where M = Co, Ni or Mn [46], [49], [50]. Furthermore, the peak in the region of 2θ= 42.37° was assigned to MnO in the cathode material [46].

3.2. *Oxidation of D-glucose using LiBBM-600 catalyst under oxygen atmosphere*

Oxidation of D-glucose was tested to evaluate the activity of LiBBM-600 catalyst under different reaction conditions in basic and neutral mediums. Reaction conditions, conversion (%) and product yields (%) in LiBBM-600 catalyzed oxidation of D-glucose under oxygen atmosphere are shown in Table 1. All reactions were carried out in 10 mg LiBBM-600/mmol of D-glucose catalyst loading. Five significant products: glycolic, tartaric, malic, succinic and 2-hydroxybutaric acid were identified in these experiments by comparison of retention times with authentic samples and further confirmed by comparing the mass spectra data with library.

Initial experiments carried out at 150 °C, 2 h, under 3.4 Atm. O_2 in 0.50 M NaOH showed 100% conversion of D-glucose and 78% yield of glycolic acid, the other minor products tartaric and succinic acids were detected in 2% yield each as shown in entry 1 in Table 1. Increasing the reaction time to 6 hr, while keeping the temperature at 150 °C reduced the glycolic acid yield to 42% (entry 2). Further experiments at 140 and 130 °C with heating times of 4 h each showed improvements in glycolic acid yield as shown in entries 3 and 4. Further reducing the reaction temperature to 120 °C and keeping the reaction time for 2 h as in entry 1 improved the glycolic acid yield to 94% and this is the highest yield achieved in the series of glucose oxidation experiments (entry 5). Reducing the temperature further to 100 ºC and oxygen pressure to 1.0 Atm. resulted a decrease in glycolic acid yield to 85%; tartaric, malic and 2-hydroxybutaric acids were observed in 3%, 1% and 2% yields respectively as shown in entry 6 of Table 1. In order to check the effect of basic medium on the reaction, the experiment in entry 6 was repeated in aqueous medium without using NaOH. However, only a 12% D-glucose conversion was observed without using NaOH (entry 7), showing the importance of 0.5 M aq. NaOH medium for effective D-glucose oxidation using LiBBM-600 catalyst.

Multifunctional catalysts combining the abilities of isomerization, dehydration, rehydration and retro-aldol fragmentation can produce a variety of C1-C6 carboxylic acid and aldehyde products in glucose oxidation reactions. In general, fragmentation of C6 sugars under anaerobic conditions gives lactic and levulinic acids; whereas under oxidative conditions are known to give glycolic, acetic and formic acids [51]. Retro-aldol reaction is proposed as a major pathway for glucose fragmentations catalyzed by Sn-β-zeolite [52], polyoxomolybdates [53], [54], Ru/C-ZnO [55], Cu-La_2O_3/Al_2O_3 [56], $VOSO_4$ [57] and Fe, Co, Mn Perovskite type oxides [58] in a number of recent glucose oxidation studies. The direct use cellulose in place of glucose is also known in these carbohydrate degradation experiments carried out under oxidative conditions [59]; where in a recent example, Zhang et al. reported a direct conversion of cellulose to glycolic acid with a phosphomolybdic acid catalyst and proposed a retro-aldol fragmentation based mechanism to explain the degradation of the glucose intermediate [59]. The proposed reaction scheme for the formation of glycolic, tartaric, malic, succinic and 2-hydroxybutaric acid from the LiBBM-600 catalyzed oxidation of D-glucose is shown in Fig. 6. The [4 + 2] retro-Aldol reaction of the open chain isomeric form of D-glucose can fragment the C6 sugar to a C4 product: erythrose (2,3,4-trihydroxybutraldehyde) and glycolaldehyde. This key intermediate erythrose possibly will further fragment into two molecules of glycolaldehyde via a [2 + 2] retro-Aldol reaction producing more glycolaldehyde. The LiBBM-600 catalyzed oxidation of glycolaldehyde gives the major product glycolic acid as shown in the top right hand corner of the scheme. The four C4 minor products tartaric, malic, succinic and 2-hydroxybutaric acid are all most likely formed from erythrose as shown in the lower half of the scheme.

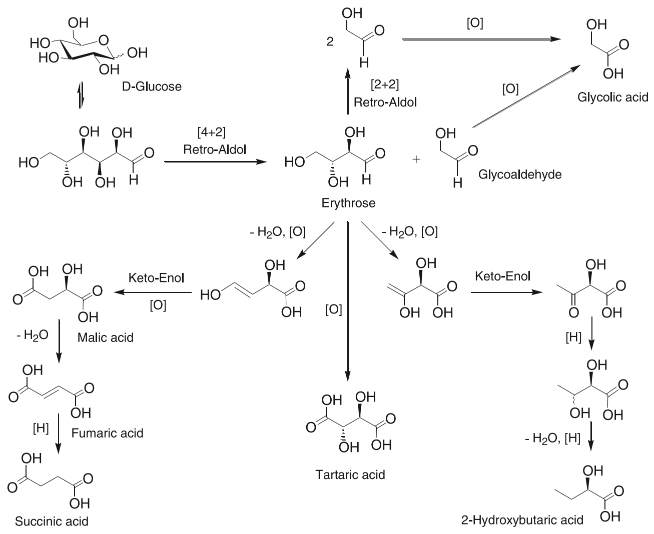

Fig. 6. Proposed pathways for the formation of glycolic, tartaric, malic, succinic and 2-hydroxybutaric acids from D-glucose in LiBBM-600 catalyzed oxidation under oxygen atmosphere in 0.5 M aqueous NaOH at 100–150 °C.

Oxidation of aldehyde and primary alcohol functions of erythrose may lead to tartaric acid. Dehydration of C3 hydroxyl group in erythrose, keto-enol tautomerism and oxidation of aldehyde functional groups is a possible path to give malic acid found as one of the minor products. Dehydration of the malic acid followed by an H-transfer reduction of intermediate fumaric acid is the likely path for the succinic acid product as shown in the lower left side of the scheme. Similarly, dehydration of C4 hydroxyl group in erythrose, keto-enol tautomerism, oxidation of aldehyde functional groups followed by reduction - dehydration - reduction is a possible path to form 2-hydroxybutaric acid as shown in the lower left corner of the scheme in Fig. 6.

In comparison of the current result with literature, catalytic oxidation of D-glucose to glycolic acid is known only in a handful of examples, and even in these instances glycolic acid was formed only as a minor product among a number of other C1-C6 glucose oxidation products [60], [7]. For example, Velarde et al. have studied the use of a series of Ti-Zeolites for oxidation of glucose using hydrogen peroxide as the oxidant; where the highest selectivity for glycolic acid was only 10.5%, and was observed with the use of Ti-MCM-41 [61]. In another example, Onda et al. have studied the D-glucose oxidation using a series transition metals: Ru, Cu, Ag, Pd and Pt on carbon catalysts in 1.0 M aq. NaOH, using air as the oxidant [7]. In this instance, highest glycolic acid selectivities of 8.7% and 5.1% were achieved with the use Cu/C and Ag/C catalysts, respectively [7]. However, relatively higher selectivity towards glycolic acid is known with acidic polyoxomolybdates, where $H_3PMo_{12}O_{40}$ was used as catalyst in water at 125 °C, producing glycolic acid in 30.1% selectivity [53]. In a recent example, Cao and co-workers have shown that D-glucose can be converted to glycolic acid in 13.58% yield by using Wells–Dawson phosphomolybdic heteropolyacid $H_6P_2Mo_{18}O_{62}$ in aqueous media at 180 °C [54]. Additional literature examples for glucose oxidation using expensive noble metal catalysts are shown in Table 2 for comparison with the presented results from this work. Evidently, the application of noble metal catalyst mostly resulted gluconic acid as the major product. Therefore, in contrast to the currently available catalytic systems for conversion of D-glucose to value added products, the new spent LiB waste material based LiBBM-600 catalyst is highly selective inexpensive or no-cost catalyst system in producing glycolic acid. This superior selectivity for glycolic acid may be due to the ability of lithium nickel manganese cobalt oxide ($Li_aNi_bMn_cCo_dO_e$) for the efficient promotion of both [4 + 2] and [2 + 2] retro-Aldol fragmentation steps as well as oxidation of glycolaldehyde to glycolic acid shown in the proposed reaction scheme in Fig. 6.

4. Conclusion

We have shown that an excellent catalyst for industrially important D-glucose to glycolic acid oxidation process can be prepared by pyrolysis of electrode coating material collected from a used Li-ion laptop battery in air at 600 °C. The new catalyst was shown to contain lithium nickel manganese cobalt oxide ($Li_aNi_bMn_cCo_dO_e$) impregnated on graphite carbon by SEM, EDX and X-ray crystallography analysis. Furthermore, the most likely active catalytic material has an empirical composition of Ni: Mn: Co 4.12: 2.10: 1.50 as indicated by the EDX data of the catalytic material. The new catalyst was tested for oxidation of D-glucose under an oxygen atmosphere of 1.0–3.4 Atm, at 100–150 °C, in water and aq. NaOH mediums with 10 mg /mmol glucose catalyst loading. The highest glucose yield of 94% was obtained for an experiment carried out at 120 °C, 2 h, under 3.4 Atm. O_2 in 0.50 M NaOH. Tartaric, malic, succinic and 2-hydroxybutaric acids were identified as minor products in D-glucose oxidation reactions. Furthermore, we have found that it is essential to use 0.5 M NaOH basic medium for the D-glucose oxidation as reactions carried out in aqueous medium under comparable conditions produced only a low 12% conversion of D-glucose. A reaction pathway is proposed to explain the formation of glycolic acid and minor C4 acid products formed in the experiments. In conclusion, we have presented a new use for spent Li-ion battery waste electrode material rich in Li, Ni, Co and Mn as a pre-fabricated catalyst for the preparation of a value added feedstock glycolic acid with numerous applications in cosmetic, food and other industries from D-glucose under mild conditions using oxygen as the oxidant. We are currently working on designing a new class of carbohydrate degradation catalysts based on this discovery and recyclability of these catalysts.

Table 2
Literature examples of glucose oxidation using expensive noble metal catalysts.

Catalyst (loading)	Reaction conditions	Product(s) (yield)	Reference
Au/ZrO_2, Au/Al_2O_3 (5%)	50 °C and pH9.0, pO_2 1 Atm.	Gluconic acid (98%)	[62]
Au/C (1%)	323–373 K, pO_2 = 100–300 kPa	Gluconic acid (63–74%)	[63]
Au–Pd/MgO_2 (0.5%)	60 °C, pO_2 = 1Atm., 24 h	Gluconic acid (62%)	[64]
Ru^{III} -^{n}Pr-NH_2-SiO_2 -^{n}Bu-NH_2 (4%)	180 °C, pO_2 = 10 bar, 2 h	Succinic acid (87.5%)	[65]
Au-C(0.8–1%)	343.2 K, pO_2 = 303.9 kPa, 0.3 M NaOH	Glycolic acid (91–94%)	[66]
Pt-Cu/TiO_2 (4–5%)	90 °C, pO_2 = 15 bar	Glucaric acid (60%)	[6]
Au-Pd/TiO_2 and Au-Pt/TiO_2 (2.5%)	160 °C, pO_2 = 3 bar, 1 h	Gluconic acid (88.6%), Glucaric acid (3.6%), Glyolic acid (0.6%)	[67]
Ru, N-doped graphene (1%)	160 °C, pO_2 = 18 atm.	Succinic acid (87%)	[68]
Au-Pt/ZrO_2 (1%)	160 °C pAir= 40 bar	Glucaric acid (50%)	[69]
Ru-MNP-MWCNT (4%)	180 °C, pO_2 = 10 atm., 6 h	Succinic acid (86%)	[70]

CRediT authorship contribution statement

Ananda S. Amarasekara: Conceptualization, Methodology, Experiments, Writing – original draft preparation. **Hashini N. K. Herath**: Experiments, Sample analysis and characterizations. **Tony L. Grady**: Sample analysis. **Cristian D. Gutierrez Reyes**: Experiments, Sample analysis and characterizations.

Declaration of Competing Interest

The authors declare that they have no known competing financial interests or personal relationships that could have appeared to influence the work reported in this paper.

Data Availability

No data was used for the research described in the article.

Acknowledgments

We thank United States National Science Foundation grants CBET-1704144, HRD-1036593, Welch Foundation grant L0002 - 20181021 and United States Department of Energy - National Nuclear Security Administration (DOE-NNSA) grant DE-NA0003947 for financial support. Dr. Sheena Reeves and Nigel Brooks are thanked for powder X-ray experiments.

References

[1] M. Rose, R. Palkovits, Macromol. Rapid Commun. 32 (2011) 1299–1311.
[2] J. Artz, R. Palkovits, Curr. Opin. Green. Sustain. Chem. 14 (2018) 14–18.
[3] A.S. Amarasekara, Handbook of Cellulosic Ethanol, John Wiley & Sons, NewYork, 2013.
[4] Q. Zhang, Z. Wan, I.K.M. Yu, D.C.W. Tsang, J. Clean. Product. 312 (2021), 127745.

[5] I. Dencic, J. Meuldijk, M. de Croon, V. Hessel, J. Flow. Chem. 1 (2012) 13–23.
[6] H. Shi, P. Thapa, B. Subramaniam, R. Chaudhari, Org. Process Res. Dev. 22 (2018).
[7] A. Onda, T. Ochi, K. Kajiyoshi, K. Yanagisawa, Appl. Catal. A: Gen. 343 (2008) 49–54.
[8] T.N. Smith, K. Hash, C.-L. Davey, H. Mills, H. Williams, D.E. Kiely, Carbohydr. Res. 350 (2012) 6–13.
[9] N. Merbouh, J.F. Thaburet, M. Ibert, F. Marsais, J.M. Bobbitt, Carbohydr. Res. 336 (2001) 75–78.
[10] X. Meng, Z. Li, D. Li, Y. Huang, J. Ma, C. Liu, X. Peng, Green. Chem. 22 (2020) 2588–2597.
[11] M.C. Ortega-Liebana, J. Bonet-Aleta, J.L. Hueso, J. Santamaria, Catalysts 10 (2020) 333.
[12] K. Shim, W.-C. Lee, Y.-U. Heo, M. Shahabuddin, M.-S. Park, M.S.A. Hossain, J. H. Kim, Sci. Rep. 9 (2019) 1–7.
[13] J. Lee, B. Saha, D.G. Vlachos, Green. Chem. 18 (2016) 3815–3822.
[14] J. Chen, Q. Ma, M. Li, D. Chao, L. Huang, W. Wu, Y. Fang, S. Dong, Nat. Commun. 12 (2021) 1–9.
[15] M. Chenouf, C. Megías-Sayago, F. Ammari, S. Ivanova, M.A. Centeno, J. A. Odriozola, Catalysts 9 (2019) 125.
[16] L. Fan, D. Lou, H. Wu, X. Zhang, Y. Zhu, N. Gu, Y. Zhang, A. Novel, Adv. Mat. Interface 5 (2018), 1801070.
[17] R. Wojcieszak, I.M. Cuccovia, M.A. Silva, L.M. Rossi, J. Mol. Catal. A: Chem. 422 (2016) 35–42.
[18] M. Comotti, C.D. Pina, M. Rossi, J. Mol. Catal. A: Chem. 251 (2006) 89–92.
[19] M. Liu, X. Jin, G. Zhang, Q. Xia, L. Lai, J. Wang, W. Zhang, Y. Sun, J. Ding, H. Yan, ACS Catal. 10 (2020) 10932–10945.
[20] C.-T. Hsieh, Y.-F. Chen, P.-Y. Yu, Int. J. Hydrog. Energ. 40 (2015) 14857–14865.
[21] H. Zhang, N. Toshima, Catal. Sci. Technol. 3 (2013) 268–278.
[22] H. Zhang, Y. Cao, L. Lu, Z. Cheng, S. Zhang, Metall. Mater. Trans. B 46 (2015) 523–530.
[23] M. Sayed, J. Yu, G. Liu, M. Jaroniec, Chem. Rev. 8 (2022) 10484–10537.
[24] R. Ge, J. Li, H. Duan, Sci. China Mat. (2022). DOI.org/10.1007/s40843-022-2076-y.
[25] M. Cao, H. Cao, W. Meng, Q. Wang, Y. Bi, X. Liang, H. Yang, L. Zhang, M.-F. Lang, J. Sun, Int. J. Hydrog. Energ. 46 (2021) 28527–28536.
[26] L. Da Vià, C. Recchi, T.E. Davies, N. Greeves, J.A. Lopez-Sanchez, ChemCatChem 8 (2016) 3475–3483.
[27] H. Yan, Q. Shen, Y. Sun, S. Zhao, R. Lu, M. Gong, Y. Liu, X. Zhou, X. Jin, X. Feng, ACS Catal. 11 (2021) 6371–6383.
[28] H. Yan, M. Zhao, X. Feng, S. Zhao, X. Zhou, S. Li, M. Zha, F. Meng, X. Chen, Y. Liu, Angewand. Chem. (2022), e202116059.
[29] A.S. Amarasekara, O.S. Owereh, Ind. Eng. Chem. Res. 48 (2009) 10152–10155.
[30] A.S. Amarasekara, C.D. Gutierrez, Renew. Energ. 136 (2019) 352–357.
[31] A.S. Amarasekara, I. McNeal, J. Murillo, D. Green, A. Jennings, Catal. Commun. 9 (2008) 2437–2440.
[32] A.S. Amarasekara, L.H. Nguyen, N.C. Okorie, S.M. Jamal, Green. Chem. 19 (2017) 1570–1575.
[33] J. Sharad, Clin., Cosmet. Invest. Dermatol. 6 (2013) 281.
[34] K.J. Jem, B. Tan, Adv. Ind. Eng. Polym. Res. 3 (2020) 60–70.
[35] L. Salusjärvi, S. Havukainen, O. Koivistoinen, M. Toivari, Appl. Microbiol. Biotechnol. 103 (2019) 2525–2535.
[36] F. Gu, J. Guo, X. Yao, P.A. Summers, S.D. Widijatmoko, P. Hall, J. Clean. Product. 161 (2017) 765–780.
[37] E. Fan, L. Li, Z. Wang, J. Lin, Y. Huang, Y. Yao, R. Chen, F. Wu, Chem. Rev. 120 (2020) 7020–7063.
[38] D.H.P. Kang, M. Chen, O.A. Ogunseitan, Environ. Sci. Technol. 47 (2013) 5495–5503.
[39] X. Zhang, L. Li, E. Fan, Q. Xue, Y. Bian, F. Wu, R. Chen, Chem. Soc. Rev. 47 (2018) 7239–7302.
[40] J. Piątek, S. Afyon, T.M. Budnyak, S. Budnyk, M.H. Sipponen, A. Slabon, Adv. Energ. Mat. 11 (2021), 2003456.
[41] X. Ma, L. Azhari, Y. Wang, Chem 7 (2021) 2843–2847.
[42] M. Scarsella, B. de Caprariis, M. Damizia, P. De Filippis, Biomass-.-. Bioenerg. 140 (2020), 105662.
[43] C. Muangsuwan, W. Kriprasertkul, S. Ratchahat, C.-G. Liu, P. Posoknistakul, N. Laosiripojana, C. Sakdaronnarong, ACS Omega 6 (2021) 2999–3016.
[44] K. Liivand, M. Kazemi, P. Walke, V. Mikli, M. Uibu, D.D. Macdonald, I. Kruusenberg, ChemSusChem 14 (2021) 1103–1111.
[45] Z. Chen, W. Zou, R. Zheng, W. Wei, W. Wei, B.-J. Ni, H. Chen, Green. Chem. 23 (2021) 6538–6547.
[46] E. Paone, M. Miceli, A. Malara, G. Ye, E. Mousa, E. Bontempi, P. Frontera, F. Mauriello, ACS Sustain. Chem. Eng. (2022).
[47] R. Botella, A. Piñeiro-García, V. Semetey, G. Lefèvre, Mater. Lett. 320 (2022), 132352.
[48] K. Xiang, S. Li, Y. Li, H. Wang, R. Xiang, Ceram. Int. 48 (2022) 23341–23347.
[49] Y. Xu, Q. Feng, K. Kajiyoshi, K. Yanagisawa, X. Yang, Y. Makita, S. Kasaishi, K. Ooi, Chem. Mat. 14 (2002) 3844–3851.
[50] A. Manthiram, J. Kim, Chem. Mat. 10 (1998) 2895–2909.
[51] W. Deng, Q. Zhang, Y. Wang, Catal. Today 234 (2014) 31–41.
[52] R. Navar, L. Botti, G. Tarantino, C. Hammond, Reactions 3 (2022) 265–282.
[53] A. Bayu, S. Karnjanakom, A. Yoshida, K. Kusakabe, A. Abudula, G. Guan, Catal. Today 332 (2019) 28–34.
[54] J. Cao, X. Wang, Y. Zhang, Chem. Eng. 7 (2022) 691–698.
[55] Y. Hirano, K. Sagata, Y. Kita, Appl. Catal. A: Gen. 502 (2015) 1–7.
[56] P. Yazdani, B. Wang, S. Rimaz, S. Kawi, A. Borgna, Mol. Catal. 466 (2019) 138–145.
[57] Z. Tang, W. Deng, Y. Wang, E. Zhu, X. Wan, Q. Zhang, Y. Wang, ChemSusChem 7 (2014) 1557–1567.
[58] S. Scelfo, F. Geobaldo, R. Pirone, N. Russo, Carbohydr. Res. 514 (2022), 108529.
[59] J. Zhang, X. Liu, M. Sun, X. Ma, Y. Han, ACS Catal. 2 (2012) 1698–1702.
[60] M. Khawaji, I. Graça, E. Ware, D. Chadwick, Catal. Today 365 (2021) 257–264.
[61] A.Mn Velarde, P. Bartl, T.E.W. Nießen, W.F. Hoelderich, J. Mol. Catal. A: Chem. 157 (2000) 225–236.
[62] T. Ishida, N. Kinoshita, H. Okatsu, T. Akita, T. Takei, M. Haruta, Angewand. Chem. 120 (2008) 9405–9408.
[63] S. Biella, L. Prati, M. Rossi, J. Catal. 206 (2002) 242–247.
[64] I. Nikov, K. Paev, Catal. Today 24 (1995) 41–47.
[65] I. Podolean, C. Rizescu, C. Bala, L. Rotariu, V.I. Parvulescu, S.M. Coman, H. Garcia, ChemSusChem 9 (2016) 2307–2311.
[66] M. Comotti, C.D. Pina, R. Matarrese, M. Rossi, A. Siani, Appl. Catal. A: Gen. 291 (2005) 204–209.
[67] Y. Cao, S. Iqbal, P.J. Miedziak, D.R. Jones, D.J. Morgan, X. Liu, J. Wang, G. J. Hutchings, J. Chem. Technol. Biotechnol. 92 (2017) 2246–2253.
[68] C. Rizescu, I. Podolean, B. Cojocaru, V.I. Parvulescu, S.M. Coman, J. Albero, H. Garcia, ChemCatChem 9 (2017) 3314–3321.
[69] E. Derrien, M. Mounguengui-Diallo, N. Perret, P. Marion, C. Pinel, M. Besson, Ind. Eng. Chem. Res. 56 (2017) 13175–13189.
[70] I. Podolean, B. Cojocaru, H. Garcia, C. Teodorescu, V.I. Parvulescu, S.M. Coman, Top. Catal. 61 (2018) 1866–1876.